η^1- and η^3-Allylpalladium(II) Complexes Bearing Potentially Tridentate Ligands: Synthesis, Solution Dynamics, and Crystal Structures

Laurent Barloy,[a] Shailesh Ramdeehul,[a] John A. Osborn,*[a][†] Claire Carlotti,[b] Francis Taulelle,[b] André De Cian,[c] and Jean Fischer[c]

Keywords: Palladium / Allyl complexes / Tridentate ligands / Fluxionality

The potentially tridentate ligands 2,2′:6′,2"-terpyridine (terpy) and 2,6-bis(diphenylphosphanylmethyl)pyridine (PNP) have been used to prepare novel palladium–allyl complexes of general formula [(terpy)Pd(CH_2CHCRR')](BF_4) [R = R′ = H (**1**); R = H, R′ = Me (**2**); R = R′ = Me (**3**)] and [(PNP)Pd(CH_2CHCRR')](BF_4) [R = R′ = H (**4**); R = H, R′ = Me (**5**); R = R′ = Me (**6**)], which were characterized by elemental analysis, IR spectroscopy, and ^{13}C, ^{31}P and variable-temperature ^1H NMR spectroscopy. The low-temperature ^1H NMR spectra show that the configuration of the complexes in solution depends strongly on the nature of the ligand. The terpy complexes **1**–**3** are η^3-allyl species, where terpy is dihapto and one pyridine ring remains uncoordinated, whereas the PNP complexes **4**–**6** occur as η^1-allyl compounds with a trihapto PNP ligand. All complexes are fluxional through η^3-η^1 exchange processes. Energy barriers of 47.5–48.6 kJ·mol^{-1} (243–262 K) are reported for the interconversion of terminal allylic protons (complexes **2**–**4**). $\Delta G^{\ddagger}$ is higher (71.1 kJ·mol^{-1} at 350 K) for the interconversion of the methyl groups in complex **6**. A lower-barrier oscillatory mechanism involving terpy ($\Delta G^{\ddagger}$ = 43.9 kJ·mol^{-1} at 231 K) is also involved in complex **1**. The X-ray structures of complexes [(η^3-terpy)Pd(η^1-C_5H_9)](BF_4) (**3a**) and [(η^3-PNP)Pd(η^1-C_4H_7)](BF_4) (**5a**) are reported; the structure of **3a** corresponds to a species that is not observed in solution.

Introduction

Palladium−allyl complexes have been much studied in the last thirty years, and have recently attracted even more attention because of their importance as intermediates in palladium-catalyzed allylic substitution (e.g. alkylation) reactions. Attack of the nucleophile on a cationic palladium η^3-allyl complex is at present conventionally accepted as the crucial step in the catalytic cycle.[1] One major goal in allylic alkylation catalysis is to achieve regio-, stereo- or enantioselectivity, especially by modifying the nature of the spectator ligand. Up to now, few examples have been reported concerning the use of potentially meridional tridentate ligands in palladium allyl chemistry[2−5] or in palladium-catalyzed allylic alkylation.[5,6] This type of ligand is prone to stabilize a η^1-allyl palladium complex, which was proposed in some cases as another possible intermediate in allylic substitution.[7]

We have lately been interested in the use of potentially tridentate ligands, such as the mixed-P,N-donor ligand 2,6-(diphenylphosphanylmethyl)pyridine (PNP) and its derivatives, in coordination chemistry and catalysis.[8] We have also reported preliminary results in palladium allyl chemistry with 2,2′:6′,2"-terpyridine (terpy).[9] Therefore we decided to investigate the influence of the nature of the tridentate ligand and the allyl ligand on the structure of the corresponding complex.

We report here the synthesis and complete characterization, especially by X-ray diffraction analysis and variable-temperature NMR spectroscopy, of palladium allyl complexes bearing the terpy and PNP ligands.

Results and Discussion

The complexes **1**−**6** were prepared in good chemical yields (73−92%) by abstraction of Cl^- from the corresponding chloride-bridged allylpalladium dimers with a silver salt, followed by coordination of palladium(II) with the appropriate ligand (Table 1). They were obtained as air-

Table 1. Synthesized palladium complexes [(ligand)-Pd(CH_2CHCRR')](BF_4)

Complex	Ligand	R	R′
1	terpy	H	H
2	terpy	H	Me
3	terpy	Me	Me
4	PNP	H	H
5	PNP	H	Me
6	PNP	Me	Me

[a] Laboratoire de Chimie des Métaux de Transition et de Catalyse, UMR 7513 CNRS, Institut Le Bel, Université Louis Pasteur, 4 rue Blaise Pascal, 67070 Strasbourg Cedex, France
Fax: (internat.) +33-388/416-171
E-mail: barloy@chimie.u-strasbg.fr
[†] Deceased April 23, 2000. Send further correspondence to L. Barloy.
[b] RMN et Chimie du Solide, UMR 7510 CNRS, Institut Le Bel, Université Louis Pasteur, 4 rue Blaise Pascal, 67070 Strasbourg Cedex, France
[c] Laboratoire de Cristallochimie et Chimie Structurale, UMR 7513 CNRS, Institut Le Bel, Université Louis Pasteur, 4 rue Blaise Pascal, 67070 Strasbourg Cedex, France
Supporting information for this article is available on the WWW under http://www.wiley-vch.de/home/eurjic or from the author.

  1434−1948/00/1212−2523 $ 17.50+.50/0

stable, yellow to red powders, which were soluble in dichloromethane or acetonitrile. If we assume that these palladium complexes are square planar, we can consider that they can adopt five possible configurations (Scheme 1). It is the purpose of our study to determine which configuration is adopted by each complex in solution and/or in the solid state.

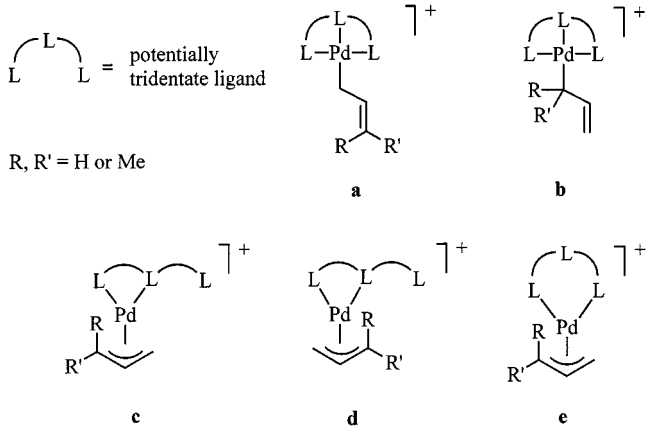

Scheme 1. Potential isomeric forms of complexes **1**−**6**

Variable-Temperature ^{1}H NMR Spectroscopy

The room-temperature ^{1}H NMR spectra of most of the synthesized complexes show some broad resonances, which is a hint that they are fluxional. Variable-temperature NMR analysis indicates that this is actually the case for all of them. It was necessary to record the spectra at low temperature (184−200 K) in order to detect the frozen species, except for complex **6**. Selected ^{1}H signals and H-H or H-P coupling constants of complexes **1**−**6** at low temperature and high or room temperature are given in Table 2 and Table 3.

The low-temperature ^{1}H NMR spectra of complexes **1**, **2**, and **3** display eleven terpy signals and five signals belonging to the allylic moiety. This pattern is characteristic of η^3-allylpalladium complexes with an unsymmetrical terpy ligand, of which only two nitrogen atoms coordinate to the metal center, viz. under the form **c** or **d** (Scheme 1). A thorough analysis shows that the actual configuration is **c**, which is also the less sterically constrained one (Scheme 2;

Table 2. ^{1}H NMR spectroscopic data for the terpy ligand in complexes **1**−**3**

Complex	T [K]	H^4/H^{18} [a]	H^5/H^{17}	H^6/H^{16}	H^7/H^{15}	H^{10}/H^{12}	H^{11}
1	298	8.81 (dt, 5.1, 1.3[b][c])	7.63 (ddd, 5.1, 7.1, 2.0[b])	8.13 (m)	8.13 (m)	8.24 (d, 7.3)	8.35 (t, 7.9)
	188	8.76 (m)	7.56 (app t, 5.9, H^{17}) 7.66 (app t, 6.1, H^5)	7.96 (m, H^{16}) 8.22 (app t, 7.6, H^6)	7.81 (d, 6.3, H^{15}) 8.40 (m, H^7)	7.96 (m, H^{12}) 8.40 (m, H^{10})	8.32 (app t, 7.9)
2	298	8.75 (d, 4.3)	7.66 (app t, 6.1)	8.13 (app t, 7.5)	8.18 (d, 8)	8.27 (d, 7.8)	8.34 (t, 7.8)
	191	8.56 (d, 5.4, H^4) 8.75 (d, 4.6, H^{18})	7.55 (app t, 6.3, H^{17}) 7.73 (app t, 6.3, H^5)	7.94 (app t, 7.8, H^{16}) 8.23 (app t, 7.9, H^6)	7.85 (br, H^{15}) 8.36 (d, 8.6, H^7)	8.01 (d, 7.2, H^{12}) 8.40 (d, 8.3, H^{10})	8.31 (app t, 7.8)
3	298	8.72 (d, 4.8)	7.69 (ddd, 5.3, 6.9, 1.4[b])	8.15 (m)	8.15 (m)	8.26 (d, 7.8)	8.34 (t, 7.8)
	200	8.54 (d, 4.8, H^4) 8.78 (d, 4.3, H^{18})	7.56 (app t, 6.0, H^{17}) 7.76 (app t, 6.3, H^5)	7.96 (app t, 7.1, H^{16}) 8.24 (app t, 7.6, H^6)	7.85 (br, H^{15}) 8.37 (d, 8.6, H^7)	8.01 (d, 7.8, H^{12}) 8.39 (d, 8.3, H^{10})	8.30 (app t, 7.8)

[a] Chemical shift data (ppm) of spectra recorded in CD_2Cl_2 on a 300 MHz (**1**) or a 400 MHz (**2**, **3**) spectrometer. For the adopted numbering scheme, see Scheme 2. Multiplicity: d = doublet, t = triplet, m = multiplet, br = broad signal, app = apparent. Numbers in parentheses are coupling constants (Hz) ($^3J_{HH}$ unless otherwise stated). − [b] $^4J_{HH}$. − [c] $^5J_{HH}$.

Table 3. ^{1}H NMR spectroscopic data for the allyl ligands in complexes **1**−**6**

Complex	T [K]	H^{2}[a]	H^1	R, R′
1	298	5.55 (quintuplet, 9.8)	3.14 (d, 9.6)	
	188	5.47 (app tt, 12.6, 6.8)	2.13 (d, 6.3, H^{syn}) 2.51 (d, 12.2, H^{anti})	3.35 (d, 12.3, H^{3anti}) 4.06 (d, 6.3, H^{3syn})
2	336[b]	5.36 (app q, 10.0)	2.83 (d, 9.1)	1.20 (d, 6.2, Me) 4.01 (dq, 10.8, 6.0, H^3)
	191[c]	5.16 (d app t, 7.0, 12.3)	2.11 (br, H^{syn})[d] 2.30 (br, H^{anti})[d]	1.40 (d, 5.9, Me) 3.86 (br, H^3)
3	298[c]	5.08 (t, 10.4)	2.51 (d, 10.2)	1.58 (s), 1.22 (s)
	200[c]	4.98 (dd, 13.1, 7.5)	2.15 (d, 6.4, H^{syn}) 2.57 (d, 13.1, H^{anti})	1.53 (s), 1.14 (s)
4	325[e]	5.67 (quintuplet t, 11.0, 1.3[f])	3.55 (d, 10.2)	
	184	5.63 (ddt, 16.3, 9.8, 8.8)	2.62 (dt, 8.4, 5.3[f])	4.18 (d, 16.4, H^{3cis}) 4.28 (d, − [g], H^{3trans})
5	325[e]	5.29 (dttq[h], 14.3, 8.4, 1.5[f], 1.5[i])	2.72 (dt, 8.6, 5.1[f])	1.12 (d, 5.5, Me) 4.83 (dq, 14.0, 5.5, H^3)
	220[j]	5.22 (dt, 14.7, 8.2)	2.62 (dt, 7.8, 5.5[f])	1.13 (d, 5.1, Me) 4.63 (dq, 14.7, 6.0, H^3)
6	298[e]	5.04 (t, 9.0)	2.70 (dt, 8.6, 4.4[f])	1.13 (s), 0.96 (s)

[a] Chemical shift data (ppm) of spectra recorded in CD_2Cl_2 on a 300 MHz spectrometer unless otherwise stated. For the adopted numbering scheme, see Scheme 2. Multiplicity: d = doublet, t = triplet, q = quadruplet, br = broad signal, app = apparent. Numbers in parentheses are coupling constants (Hz) ($^3J_{HH}$ unless otherwise stated). − [b] Solvent CD_3CN. − [c] Recorded at 400 MHz. − [d] Sharper signals at 210 K indicate J = ca. 11 Hz for H^{anti} and J = ca. 6 Hz for H^{syn}. − [e] Solvent $CDCl_3$. − [f] J_{HP} − [g] Overlap with the H^7 signal. − [h] apparent dt sextuplet. − [i] $^4J_{HH}$. − [j] Major species.

vide infra). No traces of other isomeric compounds (especially **a**) were detected at any temperature.

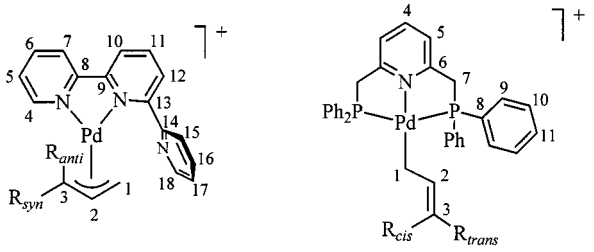

Scheme 2. Complexes present in solution according to low-temperature NMR spectroscopic data

The assignment of all signals could be made with the help of proton-decoupling experiments and/or NOE and scalar-coupling cross-peaks in 2D-ROESY NMR experiments. In fact, the aromatic pattern presents close similarities concerning both multiplicities and chemical shifts to the spectra of other bidentate terpy metal complexes analyzed in detail in the literature (Table 2, Figure 1).[10,11] The aromatic signals of complexes **1**−**3** generally appear at the same chemical shift within ±0.02 ppm at 190−200 K (Table 2). However, two protons do not follow this trend; the chemical shift of H^4 and, to a lesser extent, of H^5 are affected by the nature of the substituents R and R′. For instance, H^4 is shielded by 0.22 ppm and H^5 is deshielded by 0.1 ppm when one changes from **1** (R = R′ = H) to **3** (R = R′ = Me). This can be explained by their proximity to the R and R′ groups.

At 188 K, the H^{1anti} and H^{15} signals of **1** appear broadened; this is probably the result of a fluxional process with a very low energy barrier, i.e. the restricted rotation of the dangling pyridine. In comparison, both analogous frozen rotamers could be clearly observed by low-temperature NMR spectroscopy in the (η^2-terpy)$PtIMe_3$ complex,[10b] where the rotation is more hindered than in complex **1**. The H^1 and H^{15} signals of complexes **2** and **3** undergo the same broadening when the temperature is decreased (see Figure 1 and Figure 2); furthermore, the H^1 protons are shielded by the pendant pyridine (δ = 2.11−2.57) as they are in complex **1**.[9] These observations allow us to rule out the form **d** in favor of form **c** for the terpy complexes (Scheme 1). In the case of complex **2**, the value of the H^2-H^3 coupling constant (12.3 Hz) infers that the methyl group is in the *syn* position, which is common in η^3-allyl palladium complexes.[12]

With an increase in temperature, most of the NMR signals of complexes **1**−**3** broaden, then sharpen to give simplified spectra at or above ambient temperature. We observe the coalescence of pairs of aromatic signals H^4/H^{18}, H^5/H^{17}, H^6/H^{16}, H^7/H^{15}, and H^{10}/H^{12} characteristic of the exchange between the uncoordinating and the coordinating lateral pyridines of terpy (Table 2, Figure 1). The corresponding energy barriers were estimated from the coalescence of the clearly distinguishable H^5 and H^{17} with the help of the Eyr-

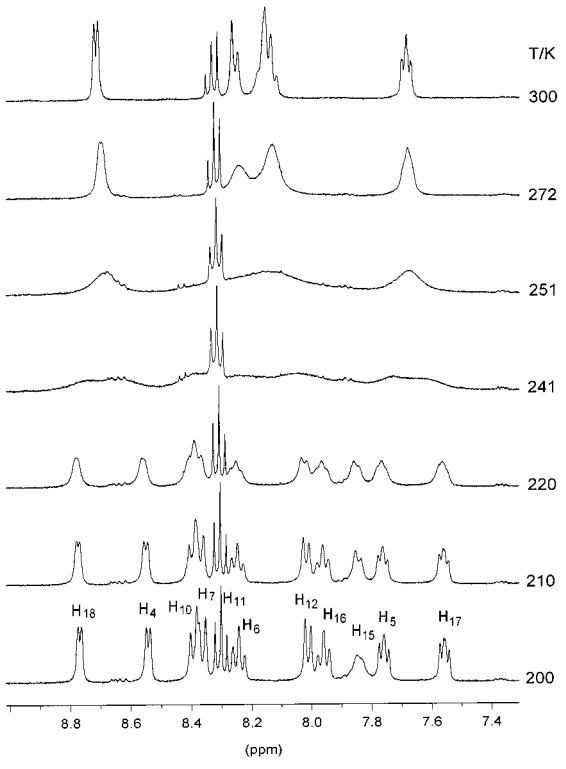

Figure 1. 400 MHz ^{1}H NMR spectra (aromatic region) of [(terpy)Pd(CH_2CHCMe_2)](BF_4) **(3)** in CD_2Cl_2 in the range 200−300 K; see Scheme 2 for hydrogen labelling

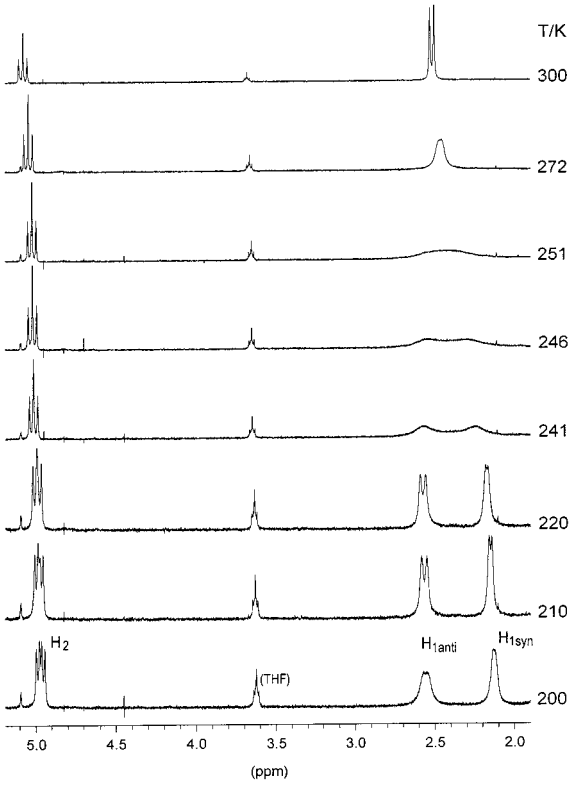

Figure 2. 400 MHz ^{1}H NMR spectra (allylic region) of [(terpy)Pd(CH_2CHCMe_2)](BF_4) **(3)** in CD_2Cl_2 in the range 200−300 K; see Scheme 2 for hydrogen labelling

ing equation (see Experimental Section), and are given in Table 4.

Table 4. Variable-temperature ^{1}H NMR spectroscopic data and calculated activation free enthalpies for fluxional processes in complexes **1**−**4** and **6**

Complex	Δν [Hz]	T_c [K]	$\Delta G^{\ddagger}$ [kJ·mol^{-1}]	Interchanging groups[a]
1[b]	29	210	43.5	H^5/H^{17}
	251	231	43.9	H^{1anti}/H^{3anti}
2[c]	72	243	48.8	H^5/H^{17}
	78	243	48.6	H^{1syn}/H^{1anti}
3[c]	81	243	48.6	H^5/H^{17}
	166	250	48.5	H^{1syn}/H^{1anti}
4[d]	807[e]	262	47.5	$H^1/(H^{3cis} + H^{3trans})$
6[f]	78	350	71.1	Me^{cis}/Me^{trans}

[a] For the adopted numbering scheme, see Scheme 2. − [b] Spectra recorded in CD_2Cl_2 at 300 MHz. − [c] Spectra recorded in CD_2Cl_2 at 400 MHz. − [d] Spectra recorded in CD_2Cl_2 at 500 MHz. − [e] Difference between the average chemical shift of H^{3cis} and H^{3trans}, and the chemical shift of H^1. − [f] Spectra recorded in [D$_6$]DMSO at 400 MHz.

The four signals corresponding to the terminal allylic protons of complex **1** coalesce into one doublet with an average coupling constant of 9.6 Hz.[9] A close examination of the NMR spectra on raising the temperature first shows a coalescence of the H^{1syn} and H^{3syn} signals and another coalescence of the H^{1anti} and H^{3anti} signals, related to a fast chemical exchange between both ends of the allyl moiety. This leads to two very large superimposed signals, which then sharpen into a doublet through a slower *syn-anti* chemical exchange. From the coalescence of both H^{anti} signals, a $\Delta G^{\ddagger}$ value of 43.9 kJ·mol^{-1} can be estimated for the first exchange; this infers that it is concerted with the exchange of the terpy hydrogens (43.5 kJ·mol^{-1}; see Table 4). This is explained by the oscillatory or "tick-tock" twist fluxional motion (Scheme 3), which was introduced by Orrell et al. for similar terpy metallic complexes[10,11] and has been the object of thorough studies and discussions.[13] In the second process, the *syn* and *anti* protons exchange through a classical η^3-η^1-η^3 mechanism,[1b] where the intermediate is probably the form **a** (Scheme 4).

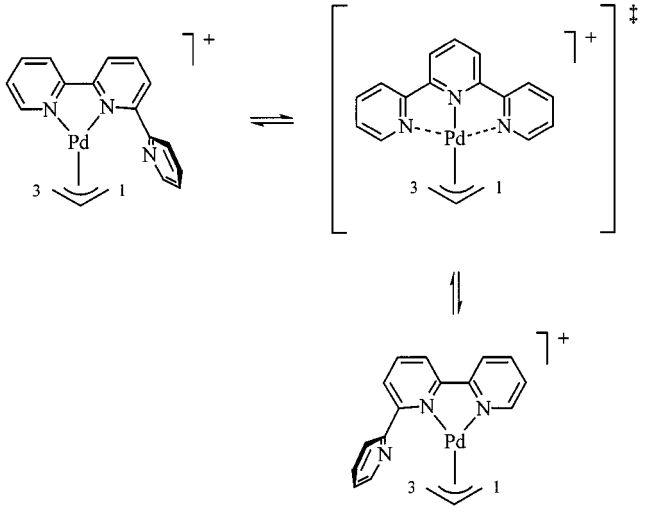

Scheme 3

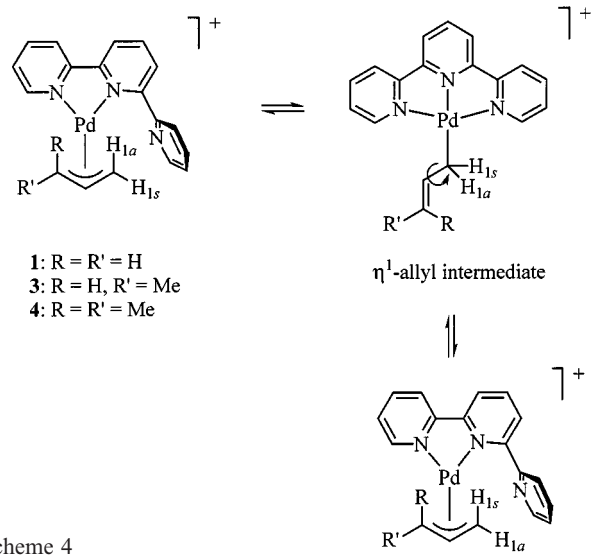

Scheme 4

A phase-sensitive 2D NMR ROESY spectrum of **1** recorded at 200 K confirms our analysis (Figure 3). Strong H^{1syn}/H^{3syn} and H^{1anti}/H^{3anti} exchange positive cross-peaks are displayed, whereas H^{syn}/H^{anti} exchange cross-peaks are not observed, perhaps because they are hidden under the geminal H^{syn}/H^{anti} NOE cross-peaks of the opposite sign. Thus the *syn*/*anti* exchanges must be slower than the *syn*/*syn* and *anti*/*anti* exchanges, otherwise the corresponding cross-peaks would probably have appeared on the ROESY spectrum in spite of the NOE effect.

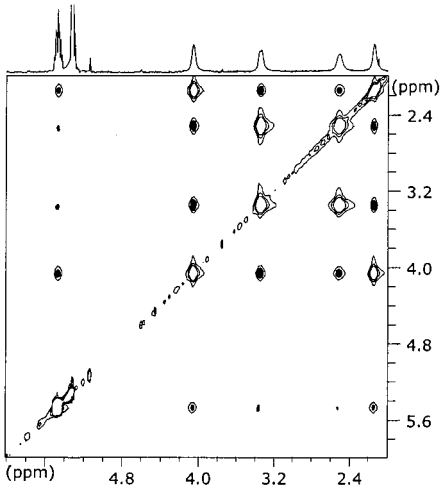

Figure 3. Section of the ^{1}H phase-sensitive ROESY spectrum of [(terpy)Pd(CH_2CHCH_2)](BF_4) **1** (CD_2Cl_2, 200 K, 500 MHz), showing exchange cross peaks and NOE (darkened) cross peaks within the allyl signals

In the spectra of complexes **2** and **3**, the two upfield H^{1syn} and H^{1anti} signals coalesce into a doublet with an average coupling constant; the H^2 signal changes from a doublet of doublets to a triplet (Figure 2). This *syn*/*anti* interconversion also takes place through the mechanism given in Scheme 4 and the corresponding energy barriers agree with the values calculated for the terpy signals (Table 4). These barriers are roughly the same for both complexes (ca.

48.6 kJ·mol^{-1}). This is not surprising if we consider that the number of substituents on the C^3 allylic carbon does not modify the steric hindrance in the intermediate involved in the fluxional process (Scheme 2). It ensues that the energy barrier of the *syn*/*anti* exchange in **1** is very likely to be approximately the same, and thus superior to the "tick-tock" barrier.

The methyl signal of **2** also undergoes some modifications over this temperature range: it broadens and sharpens several times, and this is an indication of additional fluxional processes. We believe that there are equilibria between the major isomer **c** (Me *syn*) and minor ones: isomer **c** (Me *anti*) (via the intermediate **b**) and/or isomer **d** (through the "tick-tock" mechanism) (Scheme 1). Yet the small methyl signals corresponding to these minor isomers could not be clearly distinguished in the NMR spectra. On the contrary, the methyl signals of **3** do not undergo any modification up to 340 K.

The ^{1}H NMR pattern of the PNP ligand in complexes **4**−**6** does not vary with temperature and is indicative of a tridentate coordinating mode. Apart from the aromatic signals, the methylene signal appears as a virtual triplet at δ = 4.3−4.7 (depending on the solvent and the temperature) with a $|^2J_{HP} + {}^4J_{HP'}|$ value of approximately 9 Hz. Such virtual triplets are commonly observed in the same region for other PNP palladium complexes in which the phosphorus atoms are mutually *trans*.[14,15,16]

In contrast to the terpy complexes, the allyl ligand in the frozen complexes **4**−**6** is η^1 (form **a**; see Scheme 1) according to their low-temperature (**4**,**5**) or room-temperature (**6**) NMR spectroscopic data (Table 3, Figure 4). The NMR spectra display four signals for the allyl ligand at the expected chemical shifts that one would expect by comparison with other η^1-allyl palladium complexes reported in the literature.[3,17,18] The value of the H^2-H^3 coupling constant (14.7 Hz) in complex **5** at 220 K indicates that the C−C double bond is in the thermodynamically preferred *trans* form. However, we detect a small methyl doublet at δ = 0.83 at that temperature which probably belongs to the *cis* isomer (ca. 10% according to the signal integration).

When the temperature is increased from 184 K to 325 K, the three allyl signals H^1, H^{3cis} and H^{3trans} of complex **4** coalesce into a doublet at δ = 3.55 (Figure 4). This results from a η^1-η^3-η^1 fluxional process, with an energy barrier of 47.5 kJ·mol^{-1} comparable to the ones estimated for the terpy complexes (Table 4). In complex **5**, the coalescence of the two methyl signals (T_c = 281 K) reveals that the *trans* and *cis* isomers are in equilibrium. The energy barrier calculated for the *trans* to *cis* transformation following the Shanan-Atidi and Bar-Eli method[19] reaches 60.8 kJ·mol^{-1}. We note that at high temperatures, the H^2-H^3 coupling constant is not significantly modified (ca 14 Hz, see Table 3), which suggests that the *cis* form is still minor. The methyl groups of complex **6** also exchange to give rise to a singlet at δ = 1.07 in [D_6]DMSO at high temperature; the coalescence temperature and the energy barrier are then higher (350 K and 71.1 kJ·mol^{-1}, respectively). We propose that η^3-allyl complexes and the η^1-allyl form **b** are involved as intermediates in the chemical exchanges of both complexes (see the mechanism depicted in Scheme 5). The progression of the energy barriers from **4** to **5** and **6** reflects the increasing steric hindrance within the intermediates of the fluxional processes, owing to the proximity of the methyl group(s) and the coordination sphere.

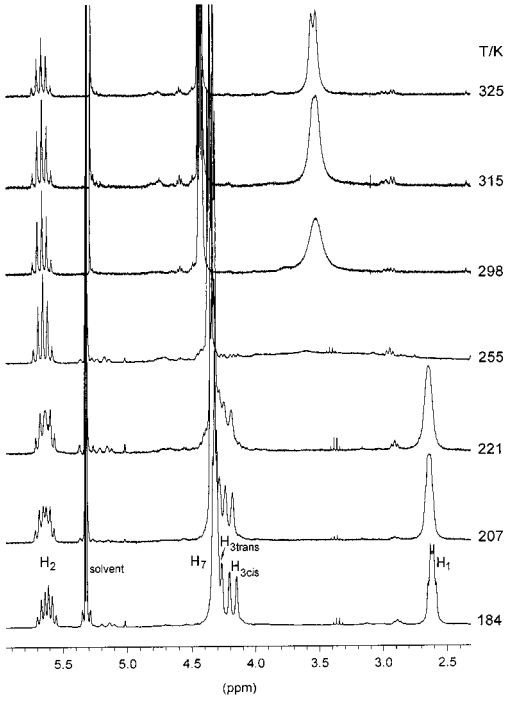

Figure 4. 300 MHz ^{1}H NMR spectra (allylic region) of [(PNP)Pd(CH_2CHCH_2)](BF_4) **(4)** (range 188−255 K: solvent CD_2Cl_2; range 298−325 K: solvent $CDCl_3$); see Scheme 2 for hydrogen labelling

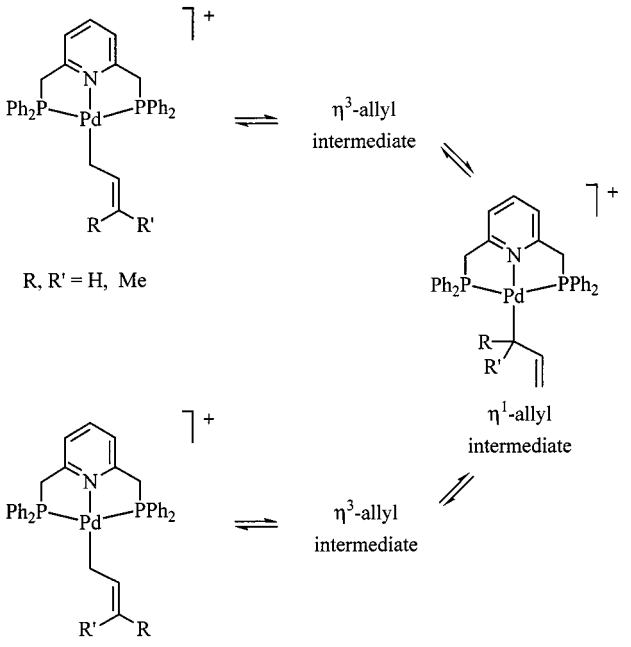

Scheme 5

Table 5. $^{13}C\{^1H\}$ NMR spectroscopic data for the complexes **1**−**6**

Complex	Me[a]	C^1/C^3	C^2	C^4/C^{18}	C^5/C^{17} + C^7/C^{15} + C^{10}/C^{12}	C^6/C^{16}	C^8/C^{14} + C^9/C^{13}	C^{11}
1		63.7	118.4	152.1	124.6, 125.3, 126.7	139.4	157.2, 158.3	141.8
2	17.1	61.3 (C^1), 81.6 (C^3)	− [b]	152.3	125.8, 126.2, 127.6	140.5	157.5, 158.3	142.5
3	26.1 22.0	58.1 (C^1), 93.5 (C^3)	112.1	150.2	124.8, 125.2, 126.8	139.5	157.3, 158.0	141.8

	Me	C^1	C^2	C^3	C^4	C^5	C^6	C^7	C^8	C^9	C^{10}	C^{11}
4[c]		− [b]	142.8	− [b]	141.5	123.8 (9)	159.5	44.6 (27)	129.2 (44)	134.3 (12)	130.5 (10)	132.9
5	18[d]	18[d]	136.0	121.4	141.5	123.8 (9)	159.4	44.7 (28)	129.5 (43)	134.4 (13)	130.5 (10)	132.9
6	17.9 (*cis*) 26.2 (*trans*)	16.1	131.5	133.5	141.4	123.7 (8)	159.2	44.7 (28)	129.7 (43)	134.3 (13)	130.4 (10)	132.8

[a] Chemical shift data (ppm) of spectra recorded at 298 K at a 50 MHz frequency (unless otherwise stated) in CD_2Cl_2 (**1**, **3**) or CD_3CN (**2**, **4**−**6**). For the adopted numbering scheme, see Scheme 2. Numbers in parentheses are coupling constants $|J_{CP} + J_{CP'}|$ (Hz) for virtual triplets. − [b] Signal not detected. − [c] 75 MHz frequency. − [d] Broad signal.

^{13}C and ^{31}P NMR Spectroscopy

In general, the proton-decoupled ^{31}P and ^{13}C NMR spectra recorded at room temperature are in agreement with the room-temperature ^1H NMR spectra, i.e. that of dynamic species (except for **6**). The ^{31}P NMR spectra of complexes **4**−**6** exhibit singlets at δ = 26.0, 25.2, and 25.1, respectively. These values are close to that found by Vasapollo and coworkers for $(PNP)PdCl_2$ (δ = 24.35), and are therefore consistent with the form **a**.[16] The room-temperature ^{13}C NMR spectroscopic data are given in Table 5. The rapidly exchanging C^1 and C^3 nuclei of **1** show a common signal at δ = 63.7. The chemical shifts for **1**, **2**, and **3** are typical of palladium η^3-allyl complexes with nitrogen-donor ligands.[20] In contrast, the vinylic carbons of the η^1-allyl complexes **4**−**6** are deshielded (δ = 121.4−142.8), whereas the C^1 signal (δ = 16.1−18) is typical of a metal-bonded carbon atom.[3c][17f] We can probably not detect the C^1/C^3 signal of **4** because the corresponding temperature of coalescence is very close to room temperature. Besides, the values found for the ^{13}C chemical shifts of the PNP ligand are consistent with the assignment proposed by Taube et al.[15]

Solid-State Analysis

We have previously reported the X-ray structures of the isomeric $[(\eta^3\text{-terpy})Pd(\eta^1\text{-}C_3H_5)]^+$ and $[(\eta^2\text{-terpy})Pd(\eta^3\text{-}C_3H_5)]^+$ cations.[9] Single crystals of **3** and **5** suitable for X-ray diffraction analysis were obtained under a nitrogen atmosphere from dichloromethane solutions by vapor-phase diffusion of diethyl ether (**3**) or pentane (**5**). Their solid-state structures are depicted in Figure 5 and Figure 6, respectively, and selected bond lengths and angles are given in Table 6 and Table 7. They crystallize as monocationic, square-planar palladium complexes and separate noncoordinating anions, and appear as the forms **3a** and **5a**, where the terpy or PNP ligand is tridentate and the allyl ligand monohapto. On the contrary, we note that the X-ray structure of the complex $[(SNS)Pd(CH_2CHCMe_2)]^+$ (SNS = 2,6-bis(dimethylthiomethyl)pyridine), resolved by Canovese et al., reveals a η^3-allyl complex with a noncoordinating sulfur.[4a] We observe a striking resemblance between the structures of $[(\eta^3\text{-terpy})Pd(\eta^1\text{-}C_3H_5)]^+$ and **3a**, which are nearly mirror images of each other, except for the C19 and C20 atoms of **3a**. The bond lengths and bond angles within the (terpy)Pd fragment are of the same order of magnitude, as well as the Pd−C16 bond length.

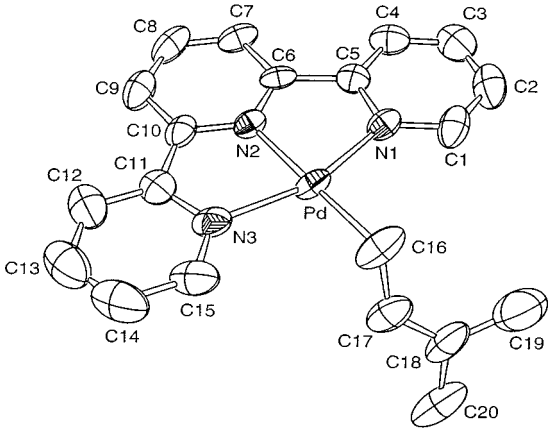

Figure 5. ORTEP drawing of **3a** showing 50% probability thermal ellipsoids and the atom-numbering scheme; hydrogen atoms and the BF_4^- anion are omitted for clarity

Two structures of **5a** are drawn in Figure 6; as long as crystallographic disorder is observed in the allyl ligand, the vinylic carbons C33 and C34 occupy two positions each. However, in both cases the allyl is in the *trans* configuration, which is also the case in the major isomer detected in solution by NMR spectroscopy (vide supra). The dihedral angles P1−Pd−C32−C33 and P1−Pd−C32−C33′ are −115.5° and −79.8°, respectively. Furthermore, the N−Pd−P1 and N−Pd−P2 bond angles are smaller than 90° [81.41(6)° and 81.61(6)°, respectively], owing to the constrained five-membered metallacycles. The palladium, nitrogen and phosphorus atoms are all nearly coplanar, with deviations of less than 0.04 Å. In general, the bond lengths and angles related to PNP and Pd compare well with the data reported for complexes $[(PNP)Pd(PEt_3)](BF_4)_2$[14] and $[(PNP)Pd(styrene)](BF_4)_2$,[15] except for the Pd−N bond length which is longer [2.137(2) Å vs. 2.107(4) and 2.058(4)

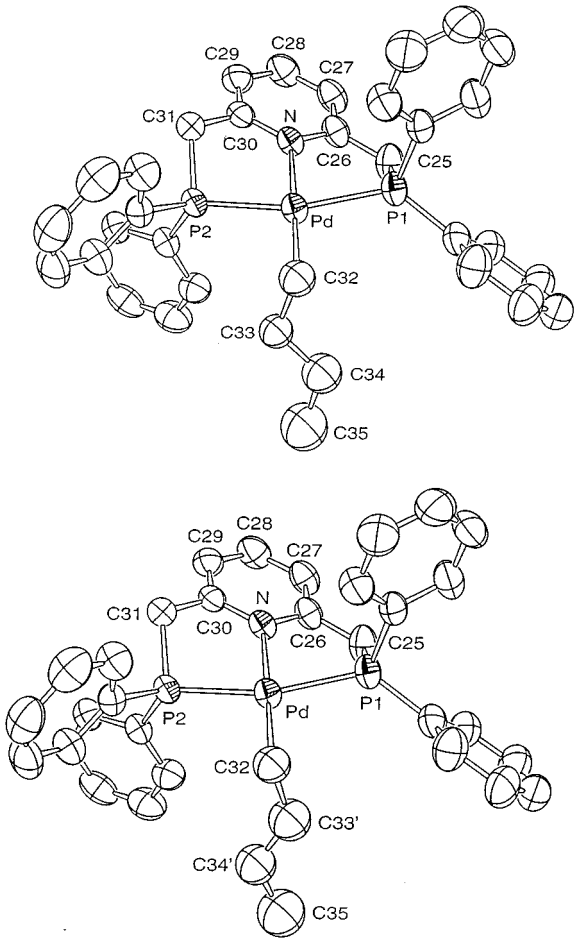

Figure 6. ORTEP drawings of both forms of **5a** showing 50% probability thermal ellipsoids and the atom-numbering scheme, the occupancy ratios for (C33, C34) and (C33′, C34′) being 50%/50%; hydrogen atoms and the BF_4^- anion are omitted for clarity

Table 6. Selected bond lengths [Å] and bond angles [°] for **3a**

Pd−N1	2.083(4)	C16−C17	1.430(9)
Pd−N2	2.017(4)	C17−C18	1.366(9)
Pd−N3	2.076(4)	C18−C19	1.49(1)
Pd−C16	2.054(6)	C18−C20	1.44(1)
N1−Pd−N2	78.6(2)	Pd−N2−C6	118.8(3)
N1−Pd−N3	158.1(2)	Pd−N2−C10	118.2(4)
N1−Pd−C16	102.1(2)	Pd−N3−C11	112.9(3)
N2−Pd−N3	79.5(2)	Pd−N3−C15	127.8(4)
N2−Pd−C16	178.2(2)	Pd−C16−C17	108.2(4)
N3−Pd−C16	99.8(2)	C16−C17−C18	131.7(7)
Pd−N1−C1	128.9(4)	C17−C18−C19	123.0(7)
Pd−N1−C5	113.7(3)	C17−C18−C20	120.5(7)

Å] because of the strong *trans* influence of the η^1-allyl ligand.[21]

The bonds lengths and bond angles of the η^1-allyl fragments of **3a** and **5a** are comparable to other examples of transition metal η^1-allyl complexes.[22] The palladium−carbon bond lengths (2.036−2.075 Å) agree with the moderate *trans* influence of pyridine.[23] We also note that the angle between the plane defined by the three allylic carbons and the coordination plane (mean plane defined by the four coordinating atoms) is roughly the same

Table 7. Selected bond lengths [Å] and bond angles [°] for **5a**

Pd−P1	2.3017(7)	C32−C33′	1.53(1)
Pd−P2	2.2894(7)	C33−C34	1.49(1)
Pd−N	2.137(2)	C34−C35	1.49(1)
Pd−C32	2.075(4)	C35−C34′	1.43(1)
C32−C33	1.425(8)	C33′−C34′	1.32(1)
P1−Pd−P2	162.76(3)	Pd−P1−C25	97.57(4)
P1−Pd−N	81.41(6)	Pd−P2−C31	98.20(3)
P1−Pd−C32	99.5(1)	Pd−C32−C33	109.8(1)
P2−Pd−N	81.61(6)	Pd−C32−C33′	106.8(2)
P2−Pd−C32	97.4(1)	C32−C33−C34	117.3(7)
N−Pd−C32	179.0(1)	C33−C34−C35	121.0(8)
Pd−N−C26	119.26(8)	C32−C33′−C34′	128.7(9)
Pd−N−C30	120.07(8)	C35−C34′−C33′	121.4(9)

for both complexes [**3a**: 109.6(6)°; **5a**: 111.9(2)° and 109.1(3)°].

Finally, a distinct medium-intensity $\nu_{C=C}$ band can be detected at approximately 1630 cm^{-1} in the IR spectra of both dimethylallyl complexes (**3**: 1629 cm^{-1}; **6**: 1634 cm^{-1}), which is characteristic of an η^1-allyl complex.[17c,24] This is consistent with the results depicted above for **6** from NMR analysis, and for **3** from X-ray diffraction studies. In addition, two bands are observed at 1599 and 1565 cm^{-1} in the spectra of complexes **4**−**6**; this confirms that the nitrogen atom of PNP actually coordinates with the palladium atom in the solid state.[25]

Conclusion

According to low-temperature NMR spectra, the complexes **1**−**3** are η^2-terpy, η^3-allyl complexes (form **c**) and the complexes **4**−**6** η^3-PNP, η^1-allyl complexes (form **a**). In no case were both forms detected together in solution (although a solution of $[(terpy)Pd(C_3H_5)]^+$ led to monocrystals of each form[9]). In comparison, Werner et al. have reported that the two isomers $[(\eta^5\text{-Cp})Pd(\eta^1\text{-}C_3H_5)]$ and $[(\eta^1\text{-Cp})Pd(\eta^3\text{-}C_3H_5)]$ coexist in solution.[18] On the basis of the six complexes studied here, the existence of one form or the other depends solely on the nature of the ancillary, potentially tridentate ligand. In contrast, whether the allyl ligand bears two, one or no methyl groups makes no difference for a given ancillary ligand.

Vrieze et al. found that $[(terpy)Pd(allyl)]^+$ adopts form **a** when the allyl bears an acetyl group in the 2 position,[3a] and that it is also the case for the (PNN)Pd(allyl) cationic complex.[3b][3c] The latter can be compared with our PNP complexes **4**−**6**, where both phosphanyl groups also show a good coordinating ability towards palladium. The presence of the form **c** is rather unexpected for our terpy complexes because of the rigidity of this ligand.[26] Indeed, the steric constraints within $[(\eta^2\text{-terpy})Pd(\eta^3\text{-}C_3H_5)]^+$ are important,[9] as indicated by various data taken from the X-ray diffraction study; thus steric factors do not seem to play a major role in the predominance of one isomeric form or another.

All complexes proved to be fluxional, as indicated by variable-temperature NMR experiments, either through a "tick-tock" mechanism or through the η^3-allyl/η^1-allyl

mechanism, which is well-known in palladium allyl chemistry. The latter reflects the competition between one donor atom of the tridentate ligand and the allylic C=C double bond to coordination to the palladium center. In our complexes, the energy barriers associated with H^{syn}/H^{anti} exchanges are lower than 50 kJ·mol^{-1}, whereas it has generally been found to be higher for allyl palladium complexes bearing mono- or bidentate ligands.[27] This is probably the effect of the tridentate nature of the ligand.

We note that only the η^3-allyl forms **1c** and **3c** could be seen in solution at 200 K, whereas the corresponding η^1-allyl isomers **1a** and **3a** were only intermediates involved in the fluxional processes. However, those intermediates can indeed be isolated in the solid state, as shown by their X-ray structures.

Experimental Section

General Remarks: All experiments were carried out under a nitrogen or argon atmosphere, using a vacuum line or Vacuum Atmospheres glovebox equipped with Dri-Train HE-493 inert gas purifier. Pentane and diethyl ether were distilled with sodium and benzophenone, and dichloromethane with calcium hydride under nitrogen immediately before use. Bis[(η^3-allyl)chloropalladium],[28] bis[(η^3-1-methylallyl)chloropalladium],[28] bis[(η^3-1,1-dimethylallyl)chloropalladium],[28] and 2,6-bis(diphenylphosphanylmethyl)pyridine[25] were prepared as described in the literature. 2,2′:6′,2"-terpyridine was purchased from Aldrich and used as received. − The NMR spectra were obtained at room temperature (unless otherwise indicated) on Bruker spectrometers, at a concentration of ca 0.02 M. ^{1}H NMR spectra were recorded at 300.16 MHz (AC-300 instrument), 400.13 MHz (AM-400) or 500.13 MHz (ARX-500) and referenced to $SiMe_4$. ^{13}C NMR{^{1}H} (broadband decoupled) spectra were recorded at 50.32 MHz (AC-200) or 75.48 MHz (AC-300) and referenced to $SiMe_4$. ^{31}P{^{1}H} (broadband decoupled) spectra were recorded at 121.51 MHz (AC-300) and referenced to 85% aqueous H_3PO_4. The assignments given are supported by irradiations or 2D NMR analysis, and/or were in agreement with ref.[29] For variable-temperature spectra, the probe temperature was controlled (±1 K) by a B-VT 2000 unit calibrated with a methanol (low-temperature) or ethylene glycol (high-temperature) NMR tube. The $\Delta G^{\ddagger}$ values were calculated with the Eyring equation[30] $\Delta G^{\ddagger} = RT_c(22.96 + \ln T_c/\Delta\nu)$ [J·mol^{-1}] where T_c (K) is the temperature of coalescence of two given signals and $\Delta\nu$ (Hz) is the difference in their chemical shifts at low exchange temperature; the error is estimated to be ±0.4 kJ·mol^{-1}. The ^{1}H phase-sensitive 2D-ROESY spectrum[31] was recorded on the ARX-500 spectrometer using a mixing time of 0.3 s. − FT-IR spectra were recorded on a Perkin−Elmer 1600 Series spectrometer on KBr pellets. − FAB MS spectra and elemental analyses were carried out by the respective facilities at the Centre de Recherche de Chimie, Université Louis Pasteur, Strasbourg.

Preparation of Complexes 1−6. Typical Procedure: To a solution of $[Pd(\eta^3\text{-}C_3H_5)Cl]_2$ (100 mg, 0.273 mmol) in CH_2Cl_2 (10 mL) was added dropwise under nitrogen and in the dark a solution of $AgBF_4$ (2.1 equiv.) in CH_2Cl_2 (2 mL). The resulting suspension was stirred at room temperature for 15 min, then filtered through celite. A solution of terpy (2.1 equiv.) in CH_2Cl_2 (2 mL) was added to the filtrate, after which the solution turned from yellow to orange. After stirring at room temperature for 15 min, the solution was evaporated to dryness and the resulting complex **1** recrystallized from CH_2Cl_2/diethyl ether as an air-stable solid.

The other complexes were prepared in a similar manner starting from the corresponding allylpalladium chloride dimer (100 mg), replacing terpy with PNP (**4**−**6**, in which case the color changed from yellow to red upon addition of the ligand) and CH_2Cl_2 with CH_3CN (**2**, **4**, **5**).

[(terpy)Pd(CH_2CHCH_2)](BF_4) (1): Orange crystals; yield 232 mg (91%). − $C_{18}H_{16}BF_4N_3Pd$ (467.55): calcd. C 46.24, H 3.45, N 8.99, found C 46.45, H 3.23, N 9.07. − MS (FAB$^+$, NBA matrix); *m/z* (%): 380.0 (100) [$M^+ - BF_4$], 339.0 (54) [$M^+ - BF_4 - C_3H_5$], 234.1 (61) terpy [$M^+ + 1$].

[(terpy)Pd($CH_2CHCHCH_3$)](BF_4) (2): Orange crystals; yield 225 mg (92%). − $C_{19}H_{18}BF_4N_3Pd\cdot1.3CH_2Cl_2$ (591.99): calcd. C 41.19, H 3.51, N 7.10, found C 41.42, H 3.43, N 6.96.

[(terpy)Pd($CH_2CHC(CH_3)_2$)](BF_4) (3): Red crystals; yield 172 mg (73%). − $C_{20}H_{20}BF_4N_3Pd$ (495.61): calcd. C 48.47, H 4.07, N 8.48, found C 48.71, H 3.90, N 8.40.

[(PNP)Pd(CH_2CHCH_2)](BF_4) (4): Orange crystals; yield 333 mg (86%). − $C_{34}H_{32}BF_4NP_2Pd$ (709.79): calcd. C 57.53, H 4.54, N 1.97, P 8.73, found C 56.35, H 4.50, N 2.07, P 8.54. − ^{31}P{^{1}H} NMR (CD_3CN, 298 K) δ = 26.0 (s). − ^{1}H NMR (300 MHz, $CDCl_3$, 325 K) δ = 4.45 (virtual t, $|^2J_{HP} + {}^4J_{HP'}|$ = 9.3 Hz, 4 H, H^7), 7.4−7.8 (m, 23 H, H^{arom}); allyl ligand signals: see Table 3.

[(PNP)Pd($CH_2CHCHCH_3$)](BF_4) (5): Yellow-orange crystals; yield 290 mg (79%). − $C_{35}H_{34}BF_4NP_2Pd$ (723.82): calcd. C 58.08, H 4.73, N 1.94, found C 57.87, H 4.77, N 2.15. − ^{31}P{^{1}H} NMR (CD_3CN, 298 K) δ = 25.2 (s). − ^{1}H NMR (300 MHz, $CDCl_3$, 325 K) δ = 4.43 (virtual t, $|^2J_{HP} + {}^4J_{HP'}|$ = 9.3 Hz, 4 H, H^7), 7.4−8.0 (m, 23H, H^{arom}); allyl ligand signals: see Table 3.

[(PNP)Pd($CH_2CHC(CH_3)_2$)](BF_4) (6): Orange crystals; yield 287 mg (82%). − $C_{36}H_{36}BF_4NP_2Pd$ (737.85): calcd. C 58.60, H 4.92, N 1.90, found C 59.14, H 4.70, N 1.77. − MS (FAB$^+$, NBA matrix); *m/z* (%): 650.1 (100) [$M^+ - BF_4$], 581.1 (81) [$M^+ - BF_4 - C_5H_9$], 504.0 (12) [$M^+ - BF_4 - C_5H_9 - Ph$]. − ^{31}P{^{1}H} NMR ([D$_6$]DMSO, 298 K) δ = 25.1 (s). − ^{1}H NMR (300 MHz, $CDCl_3$, 298 K) δ = 4.55 (virtual t, $|^2J_{HP} + {}^4J_{HP'}|$ = 9.2 Hz, 4 H, H^7), 7.4−7.8 (m, 23 H, H^{arom}); allyl ligand signals: see Table 3.

Collection of the X-ray Data and Structure Determination for 3a and 5a: For compound **3a**, a Philips PW100/16 diffractometer was used with Cu-K_α graphite monochromated radiation (λ = 1.5418 Å). For compound **5a**, the data were collected on a Nonius CAD4 or MACH3 diffractometer using Mo-K_α graphite monochromated radiation (λ = 0.7107 Å). The structures were solved by direct methods and refined against |*F*|. Hydrogen atoms were introduced as fixed contributors. Absorption corrections were derived from psi scans of 7 reflections. For all computations, the Nonius OpenMoleN package[32] was used. The crystal and refinement data are summarized in Table 8. The C32, C33, C33′, C34, C34′, and C35 atoms of **5a** were refined isotropically. Crystallographic data (excluding structure factors) for the structures reported in this paper have been deposited with the Cambridge Crystallographic Data Centre as supplementary publication no. CCDC-140659 (**3a**) and -140660 (**5a**). Copies of the data can be obtained free of charge on application to CCDC, 12 Union Road, Cambridge CB2 1EZ, UK [Fax: (internat.) + 44-1223/336-033; E-mail: deposit@ccdc.cam.ac.uk).

Table 8. Crystal and refinement data for **3a** and **5a**

Compound	**3a**	**5a**
Formula	$C_{20}H_{20}BN_3F_4Pd$	$C_{35}H_{34}BNF_4P_2Pd$
Mol wt	495.6	723.8
Color	red	yellow
Crystal system	monoclinic	triclinic
a (Å)	15.680(4)	9.763(2)
b (Å)	17.430(4)	10.532(3)
c (Å)	7.077(3)	17.085(5)
α (deg)		97.03(2)
β (deg)	90.42(2)	104.26(2)
γ (deg)		101.55(2)
V (Å^3)	1934.1	1640.7
Z	4	2
D_{calc} (g cm^{-3})	1.70	1.465
Wavelength (A)	1.54184	0.7107
μ (cm^{-1})	81.82	7.001
Space group	P 1 2_1/n 1	P−1
Diffractometer	Philips PW1100/16	Nonius Mach3
Crystal dimensions (mm)	0.30 × 0.30 × 0.25	0.40 × 0.35 × 0.35
Temperature (K)	173	293
Radiation	Cu-*Kα*, graphite monochromated	Mo-*Kα*, graphite monochromated
Mode	θ/2θ	θ/2θ
Scan speed (deg s^{-1})	0.020	variable
Scan width (deg)	0.80 + 0.14 tan θ	0.81 + 0.34 tan θ
Octants	±h+k+l	+h±k±l
θ min/max (deg)	3/54	2/30
No. of data collected	2645	10391
No. of data with $I>3\sigma(I)$	2056	6616
No. of variables	262	385
Abs min/max	0.83/1.45	0.95/1.00
R (F)	0.041	0.041
R_w (F)	0.059	0.062
Largest peak in final difference (e Å^{-3})	0.628	0.872
GOF	1.187	1.194

Acknowledgments

We thank Jean Pierre Le Ny and Alain Dedieu for helpful discussions, Roland Graff for 2D NMR analysis and Nathalie Kyritsakas for X-ray analysis. We are grateful to the Centre National de la Recherche Scientifique for supporting this work. S. R. is indebted to the Ministère de l'Education et de la Recherche Scientifique for a grant.

[1] [1a] J. Tsuji, *Tetrahedron* **1986**, *42*, 4361. – [1b] G. Consiglio, R. M. Waymouth, *Chem. Rev.* **1989**, *89*, 257. – [1c] S. A. Godleski, in: *Comprehensive Organic Synthesis* (Eds.: B. M. Trost, I. Fleming), Pergamon Press, Oxford, U. K., **1991**, vol. 4, p. 585. – [1d] C. G. Frost, J. Howarth, J. M. J. Williams, *Tetrahedron: Asymmetry* **1992**, *3*, 1089. – [1e] B. M. Trost, D. L. Van Vranken, *Chem. Rev.* **1996**, *96*, 395.

[2] P. K. Byers, A. J. Canty, *J. Chem. Soc., Chem. Commun.* **1988**, 639.

[3] [3a] R. E. Rülke, D. Kliphuis, C. J. Elsevier, J. Fraanje, K. Goubitz, P. W. N. M. van Leeuwen, K. Vrieze, *J. Chem. Soc., Chem. Commun.* **1994**, 1817. – [3b] P. Wehman, R. E. Rülke, V. E. Kaasjager, P. C. J. Kamer, H. Kooijman, A. L. Spek, C. J. Elsevier, K. Vrieze, P. W. N. M. van Leeuwen, *J. Chem. Soc., Chem. Commun.* **1995**, 331. – [3c] R. E. Rülke, V. E. Kaasjager, P. Wehman, C. J. Elsevier, P. W. N. M. van Leeuwen, K. Vrieze, J. Fraanje, K. Goubitz, A. Spek, *Organometallics* **1996**, *15*, 3022.

[4] [4a] L. Canovese, F. Visentin, P. Uguagliati, V. Lucchini, G. Bandoli, *Inorg. Chim. Acta* **1998**, *277*, 247. – [4b] L. Canovese, F. Visentin, G. Chessa, A. Niero, P. Uguagliati, *Inorg. Chim. Acta* **1999**, *293*, 44.

[5] G. Zhu, M. Terry, X. Zhang, *Tetrahedron Lett.* **1996**, *37*, 4475.

[6] [6a] J. M. Longmire, X. Zhang, *Tetrahedron Lett.* **1997**, *38*, 1725. – [6b] G. Chelucci, V. Caria, A. Saba, *J. Mol. Catal. A* **1998**, *130*, 51.

[7] [7a] B. Åkermark, G. Åkermark, L. Hegedus, K. Zetterberg, *J. Am. Chem. Soc.* **1983**, *103*, 3037. – [7b] J. C. Fiaud, J. L. Malleron, *Tetrahedron Lett.* **1981**, *22*, 1399.

[8] [8a] R. Sablong, C. Newton, P. Dierkes, J. A. Osborn, *Tetrahedron Lett.* **1996**, *37*, 4933. – [8b] R. Sablong, J. A. Osborn, *Tetrahedron Lett.* **1996**, *37*, 4937. – [8c] L. Barloy, S. Y. Ku, J. A. Osborn, A. De Cian, J. Fischer, *Polyhedron* **1997**, *16*, 291. – [8d] N. Rahmouni, J. A. Osborn, A. De Cian, J. Fischer, A. Ezzamarty, *Organometallics* **1998**, *17*, 2470.

[9] S. Ramdeehul, L. Barloy, J. A. Osborn, A. De Cian, J. Fischer, *Organometallics* **1996**, *15*, 5442.

[10] [10a] E. R. Civitello, P. S. Dragovitch, T. B. Karpishin, S. G. Novick, G. Bierach, J. F. O'Connell, T. D. Westmoreland, *Inorg. Chem.* **1993**, *32*, 237. – [10b] E. W. Abel, V. S. Dimitrov, N. J. Long, K. G. Orrell, A. G. Osborne, V. Sik, M. B. Hursthouse, M. A. Mazid, *J. Chem. Soc., Dalton Trans.* **1993**, 291. – [10c] E. W. Abel, V. S. Dimitrov, N. J. Long, K. G. Orrell, A. G. Osborne, H. M. Pain, V. Sik, M. B. Hursthouse, M. A. Mazid, *J. Chem. Soc., Dalton Trans.* **1993**, 597. – [10d] E. W. Abel, K. G. Orrell, A. G. Osborne, H. M. Pain, V. Sik, M. B. Hursthouse, K. M. Abdul Malik, *J. Chem. Soc., Dalton Trans.* **1994**, 3441.

[11] [11a] E. W. Abel, N. J. Long, K. G. Orrell, A. G. Osborne, H. M. Pain, V. Sik, *J. Chem. Soc., Chem. Commun.* **1992**, 303. – [11b] E. W. Abel, K. G. Orrell, A. G. Osborne, H. M. Pain, V. Sik, *J. Chem. Soc., Dalton Trans.* **1994**, 111.

[12] A. Vitagliano, B. Åkermark, S. Hansson, *Organometallics* **1991**, *10*, 2592.

[13] [13a] E. Rotondo, G. Giordano, D. Minniti, *J. Chem. Soc., Dalton Trans.* **1996**, 253. – [13b] E. W. Abel, K. G. Orrell, A. G. Osborne, H. M. Pain, V. Sik, M. B. Hursthouse, K. M. Abdul Malik, *J. Chem. Soc., Dalton Trans.* **1996**, 253. – [13c] E. W. Abel, A. Gelling, K. G. Orrell, A. G. Osborne, V. Sik, *Chem. Commun.* **1996**, 2329. – [13d] A. Gelling, K. G. Orrell, A. G. Osborne, V. Sik, *J. Chem. Soc., Dalton Trans.* **1998**, 937.

[14] B. D. Steffey, A. Miedaner, M. L. Maciejewski-Farmer, P. R. Bernatis, A. M. Herring, V. S. Allured, V. Carperos, D. L. DuBois, *Organometallics* **1994**, *13*, 4844.

[15] C. Hahn, A. Vitagliano, F. Giordano, R. Taube, *Organometallics* **1998**, *17*, 2060.

[16] G. Vasapollo, C. F. Nobile, A. Sacco, *J. Organomet. Chem.* **1985**, *296*, 435.

[17] [17a] J. Powell, B. L. Shaw, *J. Chem. Soc (A)* **1967**, 1839. – [17b] D. J. Tune, H. Werner, *Helv. Chim. Acta* **1975**, *58*, 2240. – [17c] S. Numata, R. Okawara, H. Kurosawa, *Inorg. Chem.* **1977**, *16*, 1737. – [17d] B. Henc, P. W. Jolly, R. Salz, S. Stobbe, G. Wilke, R. Benn, R. Mynott, K. Seevogel, R. Goddard, C. Krüger, *J. Organomet. Chem.* **1980**, *191*, 449. – [17e] H. Werner, G. T. Crisp, P. W. Jolly, H.-J. Kraus, C. Krüger, *Organometallics* **1983**, *2*, 1369. – [17f] R. Benn, P. W. Jolly, R. Mynott, B. Raspel, G. Schenker, K.-P. Schick, G. Schroth, *Organometallics* **1985**, *4*, 1945. – [17g] J. Krause, W. Bonrath, K. R. Pörschke, *Organometallics* **1992**, *11*, 1158.

[18] [18a] H. Werner, A. Kühn, *Angew. Chem. Int. Ed. Engl.* **1979**, *18*, 416. – [18b] H. Werner, A. Kühn, C. Burschka, *Chem. Ber.* **1980**, *113*, 2291.

[19] H. Shanan-Atidi, K. H. Bar-Eli, *J. Phys. Chem.* **1970**, *74*, 961.

[20] [20a] J. Herrmann, P. S. Pregosin, R. Salzmann, A. Albinati, *Organometallics* **1995**, *14*, 3311. – [20b] B. Akermark, B. Krakenberger, S. Hansson, A. Vitagliano, *Organometallics* **1987**, *6*, 620.

[21] T. G. Appleton, H. C. Clark, L. E. Manzer, *Coord. Chem. Rev.* **1973**, *10*, 335.

[22] [22a] F. Dahan, C. Agami, J. Levisalles, F. Rose-Munch, *J. Chem. Soc., Chem. Commun.* **1974**, 505. – [22b] F. Dahan, *Acta Cryst.* **1976**, *B32*, 1941. – [22c] M. A. Bennett, R. N. Johnson, G. B. Robertson, I. B. Tomkins, P. O. Whimp, *J. Am. Chem. Soc.* **1976**, *98*, 3514. – [22d] H. M. Büch, P. Binger, R. Benn, C. Krüger, A. Rufinska, *Angew. Chem. Int. Ed. Engl.* **1983**, *22*, 774. – [22e] P. W. Jolly, *Angew. Chem. Int. Ed. Engl.* **1985**, *24*, 283. – [22f] A. Döhring, R. Goddard, G. Hopp, P. W. Jolly, N. Kokel, C. Krüger, *Inorg. Chim. Acta* **1994**, *222*, 179. – [22g] T. Sone, S. Ozaki, N. C. Kasuga, A. Fukuoka, S. Komiya, *Bull. Chem. Soc. Jpn.* **1995**, *68*, 1523.

[23] B. A. Markies, D. Kruis, M. H. P. Rietveld, K. A. N. Verkerk,

J. Boersma, H. Kooijman, M. T. Lakin, A. L. Spek, G. van Koten, *J. Am. Chem. Soc.* **1995**, *117*, 5263.

[24] [24a] L. J. Bellamy, *The Infra-Red Spectra of Complex Molecules*, Methuen, London, U. K., **1964**, p. 35. – [24b] C. Sourisseau, B. Pasquier, *J. Organomet. Chem.* **1972**, *39*, 51.

[25] W. V. Dahlhoff, S. M. Nelson, *J. Chem. Soc. (A)* **1971**, 2184.

[26] R. E. Rülke, I. M. Han, C. J. Elsevier, K. Vrieze, P. W. N. M. van Leeuwen, C. F. Roobeek, M. C. Zoutberg, Y. F. Wang, C. H. Stam, *Inorg. Chim. Acta* **1990**, *169*, 5.

[27] [27a] J. W. Faller, M. E. Thomsen, M. J. Mattina, *J. Am. Chem. Soc.* **1971**, *93*, 2642. – [27b] S. Hansson, P.-O. Norrby, M. P. T. Sjögren, B. Akermark, M. E. Cucciolito, F. Giordano, A. Vitagliano, *Organometallics* **1993**, *12*, 4940. – [27c] C. Breutel, P. S. Pregosin, R. Salzmann, A. Togni, *J. Am. Chem. Soc.* **1994**, *116*, 4067. – [27d] B. Crociani, S. Antonaroli, M. Paci, F. Di Bianca, L. Canovese, *Organometallics* **1997**, *16*, 384.

[28] [28a] W. T. Dent, R. Long, A. J. Wilkinson, *J. Chem. Soc.* **1964**, 1585. – [28b] P. R. Auburn, P. B. Mackenzie, B. Bosnich, *J. Am. Chem. Soc.* **1985**, *107*, 2046.

[29] R. M. Silverstein, F. X. Webster, *Spectrometric Identification of Organic Compounds*, J. Wiley & Sons, New-York, U. S. A., **1998**.

[30] H. Günther, *La Spectroscopie de RMN*, Masson, Paris, France, **1993**.

[31] D. G. Davis, A. Bax, *J. Magn. Res.* **1985**, *64*, 533.

[32] C. K. Fair in *MolEN. "An Interactive Intelligent System for Crystal Structure Analysis"* Nonius, Delft, The Netherlands, **1990**.

Received February 18, 2000
[I00068]